AIAA 80-0802R

Vibrations of Laminated Filament-Wound Cylindrical Shells

J. B. Greenberg* and Y. Stavsky†
Technion—Israel Institute of Technology, Haifa, Israel

The equations of motion, derived from a Love-type theory, are presented for laminated filament-wound cylindrical shells in which each layer is permitted an arbitrary fixed fiber orientation. A general method of solution is established, based upon the use of a complex finite Fourier transform. The frequency spectra of free natural vibrations are investigated for numerous single, bi- and tri-layered clamped or simply supported generally orthotropic shells. The effect of fiber orientation on the frequency response is found to be quite considerable in certain composite shells; for some shells the frequency is increased by a factor of 3.1 by simply choosing an optimal combination of fiber winding angles. Similar important effects are noted due to the combined action of shell heterogeneity and fiber winding angle.

Nomenclature

a	= radius of reference surface of cylindrical shell
A_{ij}, A	= extensional stiffnesses and matrix
B_{ij}, B	= bending-extension coupling stiffnesses and matrix
$c_j^{(n)}$	= constants in Eq. (12)
D_{ij}, D	= bending stiffnesses and matrix
$D^{(n)}, D_{ij}^{(n)}$	= differential operators
E_{ij}	= elastic stiffness moduli
f	= function
F	= Fourier transform
F_e	= efficiency factor
h, h_i	= shell thickness, thickness of ith layer
I	= identity matrix
I	= increase factor
ℓ	= length of cylindrical shell
$L_{ij}, L_{ij}^{(n)}$	= differential and transformed differential operators
M_i	= M_ξ, M_θ; axial and circumferential moments
$M_{\xi\theta}$	= twisting moment
n	= circumferential mode number
N_i	= N_ξ, N_θ; axial and circumferential forces
$N_{\xi\theta}$	= shear force
R_0, R_1, R_2	= inertia terms
t	= time
u, v, w	= shell displacements
$U_i, U_i^{(n)}$	= separated shell displacements and transformed displacements
ϵ_i	= $\epsilon_\xi, \epsilon_\theta$; axial and circumferential strains
$\epsilon_{\xi\theta}$	= shear strain
ζ	= thickness coordinate
θ	= circumferential coordinate
λ	= frequency of vibration
$\mu_j^{(n)}$	= roots of polynomial auxiliary equation
ν_{12}	= Poisson's ratio
ξ	= nondimensional axial coordinate
ρ	= density
τ	= τ_ξ, τ_θ; stress components in axial and circumferential directions, respectively
$\tau_{\xi\theta}$	= shear stress
ϕ	= fiber winding angle
$\Phi^{(n)}$	= displacement function
Ω	= normalized frequency

Received March 10, 1980; presented as Paper 80-0802 at the AIAA/ASME/ASCE/AHS 21st Structures, Structural Dynamics and Materials Conference, Seattle, Wash., May 12-14, 1980; revision received Jan. 15, 1981.

*Lecturer, Department of Aeronautical Engineering.
†Gerard Swope Professor of Mechanics, Department of Aeronautical Engineering. Visiting Professor, Mechanics and Structures Dept., UCLA, Los Angeles, Calif., 1981. Member AIAA.

I. Introduction

THE growing use of filamentary composite cylindrical shells in a variety of aircraft and missile structures has engendered much interest in their theoretical analysis. However, with regard to the free vibrations problem for such shells, little reported work has appeared in the literature. As far as isotropic or orthotropic homogeneous shells are concerned, many studies of their natural frequencies have been published (see the detailed survey of Leissa[1]). For laminated orthotropic cylindrical shells, a Donnell type theory was given by Dong[2] and a refined Love-type theory of motion was formulated by Stavsky and Loewy.[3] In the latter work the frequency spectra of free natural vibrations were obtained from a closed form solution for simply supported (SS3) finite length shells. The results indicated that Donnell-type theory is inadequate in many instances and that shell orthotropy and heterogeneity can affect significantly the vibrational response of the system.

The more general problem associated with aerolotropic layups has received scant attention. Kunukasseril[4] considered such shells, but his solutions are restricted to infinitely long shells and to two special models for finite shells. For the latter shells an exact analysis was performed for the axisymmetric mode which is seldom associated with the lowest frequency, whereas an approximate analysis is given for inextensional vibrations.

Bert et al.[5] examined the nonsymmetric modes of vibration of an arbitrarily layered general anisotropic finite length shell. However, exact results are presented only for orthotropic cases, whereas for anisotropic shells an approximate method is developed in which two helical type modes are combined to satisfy the primary boundary condition (w = radial displacement = 0) at each end of the shell.

It would seem that no analytic solution has been reported for a finite shell subject to the classical simply supported or clamped boundary conditions. The difficulty in solving for the general vibrations of such anisotropic shells, even for the SS3 boundary conditions, stems from the occurrence of the shear coupling terms that prevent the appearance of the chessboard mode of vibration present in orthotropic or isotropic shells.

In the present study the work of Stavsky and Loewy[3] is extended to cover the vibrations of generally orthotropic (sometimes called aeolotropic) laminated cylindrical shells. The equations of motion, as derived from a Love-type theory, are presented for these layered shells in which each layer is permitted an arbitrary fixed fiber orientation. In the last section, calculated results are discussed and important effects of filament winding on the vibrational characteristics of such laminated shells are noted.

II. Equations of Motion

Consider a finite circular cylindrical shell made of layers of filament-wound orthotropic materials whose elastic

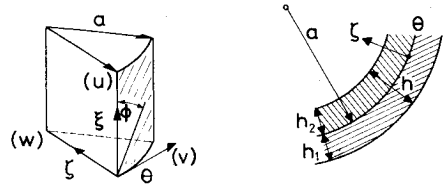

Fig. 1 Cylindrical shell notation.

properties are thickness dependent only. The nondimensional axial coordinate ξ, the circumferential coordinate θ, and the normal ζ to the reference surface (of radius a) are illustrated in Fig. 1. The winding angle of each material (i.e., the orientation of the fiber direction to the axial direction) is denoted by ϕ. A generally orthotropic construction such as this is quite common in structures built of filamentary composite materials.

A. Strain-Displacement and Stress-Strain Relations

If Love's first approximation shell theory is applied, the strains and displacements vary linearly with the thickness coordinate ζ, and the relevant details are unchanged from the development given by Stavsky and Loewy.[3] A similar remark is applicable to the dynamic equations. The point of departure from Ref. 3 for the generally orthotropic laminates relates to the stress-strain relations. Hooke's law for a generally orthotropic shell is written in terms of the elastic stiffness moduli

$$\begin{bmatrix} \epsilon_\xi \\ \tau_\theta \\ \tau_{\xi\theta} \end{bmatrix} = \begin{bmatrix} E_{\xi\xi} & E_{\xi\theta} & E_{\xi s} \\ & E_{\theta\theta} & E_{\theta s} \\ \text{sym} & & E_{ss} \end{bmatrix} \begin{bmatrix} \epsilon_\xi \\ \epsilon_\theta \\ \epsilon_{\xi\theta} \end{bmatrix} \tag{1}$$

where, in general, $E_{\xi s}$, $E_{\theta s}$ are nonzero because arbitrary fiber orientation is permitted. The case of regular orthotropy[3] causes the $E_{\xi s}$, $E_{\theta s}$ elements of E to become zero, leading to considerable mathematical simplification. As a consequence of Eq. (1) the stress-strain relations for the shell are

$$\begin{bmatrix} N \\ M \end{bmatrix} = \begin{bmatrix} A & B \\ B & D \end{bmatrix} \begin{bmatrix} \epsilon^0 \\ K \end{bmatrix} \tag{2}$$

where the elements of the full 3×3 symmetric stiffness matrices A, B, D are defined by

$$(A_{ij},B_{ij},D_{ij}) = \int_{h_1}^{h_2} E_{ij}(1,\zeta,\zeta^2)\,d\zeta \qquad (i=\xi,\theta,s) \tag{3}$$

and the superscript 0 in ϵ refers to reference surface ($\zeta=0$) values. The stress resultants and couples are defined by Stavsky and Loewy.[3]

B. Displacement Equations of Motion

The displacement equations of motion are derived by substituting from Eq. (2) into the dynamic equations of motion.[3] Furthermore, the reference surface displacements u^0,v^0,w^0 are assumed small so that their spatial and temporal variations can be separated in the usual fashion

$$(u^0,v^0,w^0) = \text{Re}\{(U_1,U_2,U_3)e^{i\lambda t}\} \tag{4}$$

where Re denotes the real part of and the U_i are functions of ξ and θ. Use of Eq. (4) in the equation of motion produces an eighth-order system of three simultaneous linear, constant coefficient, partial differential equations.

$$\sum_{j=1}^{3} L_{ij}U_j = 0 \qquad (i=1,2,3) \tag{5}$$

The functional operators L_{ij} are listed in the Appendix.

III. Solution of Eigenvalue Problem

The approach that has usually been adopted to determine the eigenvalues of particular examples of Eq. (5) (e.g., isotropic or orthotropic shells) is known as the inverse method. Details are given in various references.[6-8] In the present work a more general direct method for tackling Eq. (5) is presented. Although consideration will be given here to the problem of free vibrations only, the methodology is equally (and readily) applicable to static and stability problems for general shells of revolution.

A. Transformation of Displacement Equations

Let the finite complex Fourier integral of a function $f(\xi,\theta)$ be denoted by

$$F\{f(\xi,\theta)\} = \int_{-\pi}^{+\pi} f(\xi,\theta)e^{in\theta}\,d\theta = f^{(n)}(\xi) \tag{6}$$

where $i=\sqrt{-1}$ and n is a positive integer. If the function $f(\xi,\theta)$ and its derivatives are periodic in the circumferential direction θ then the following result is obtained

$$F\left\{\frac{\partial^s f}{\partial\theta^2}\right\} = (-in)^2 f^{(n)}(\xi) \tag{7}$$

Multiply Eq. (5) by $e^{in\theta}$ and integrate between the limits $(-\pi,\pi)$ with respect to θ. Then, with the help of Eq. (7) (because the displacement functions are periodic in the circumferential direction) a set of ordinary differential equations for the transformed displacements, $U_i^{(n)}(\xi)$ is produced.

$$\sum_{j=1}^{3} L_{ij}^{(n)} U_j^{(n)}(\xi) = 0 \qquad (i=1,2,3) \tag{8}$$

where $L_{ij}^{(n)}$ are the transformed *ordinary* differential operators.

B. Analytic Solution of Transformed Displacement Equations

The operators $L_{ij}^{(n)}$ are linear and have constant (sometimes complex) coefficients. Thus, following Ambartsumyan,[9] it can be shown that the transformed displacements are given by

$$[U_1^{(n)},U_2^{(n)},U_3^{(n)}] = [D_{31}^{(n)},D_{32}^{(n)},D_{33}^{(n)}]\Phi^{(n)} \tag{9}$$

where the displacement function $\Phi^{(n)}$ is the solution of the homogeneous equation

$$D^{(n)}\Phi^{(n)} = 0 \tag{10}$$

with the operator $D^{(n)}$ being given by

$$D^{(n)} = \det(L_{ij}^{(n)}) \tag{11}$$

The operators $D_{ij}^{(n)}$ in Eq. (9) are minors of $D^{(n)}$. The operator $D^{(n)}$ is of eighth order in the general case so that the solution of Eq. (10) is of the form

$$\Phi^{(n)} = \sum_{j=1}^{8} c_j^{(n)} e^{\mu_j^{(n)}\xi} \tag{12}$$

where $c_j^{(n)}$ are constants and the $\mu_j^{(n)}$ (here assumed distinct) are the roots of the eighth-order polynomial auxiliary equation. The eight arbitrary constants are determined from the transformed boundary conditions, four at each end of the cylinder. Finally, the actual physical displacements are recovered by operating on Eq. (9) with the inverse transformation F^{-1} and extracting the real part of the result.

If the free vibrations frequency is sought, the requirement of a nontrivial solution leads to a nonanalytic determinantal equation for λ. The natural frequency is determined by solving this equation for all positive values of n and selecting the lowest frequency computed.

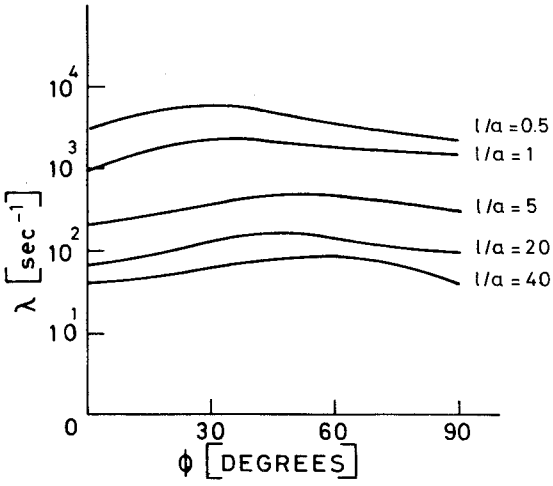

Fig. 2 Effect of fiber winding angle on frequencies of UHMG cylindrical shells; clamped-clamped boundary conditions.

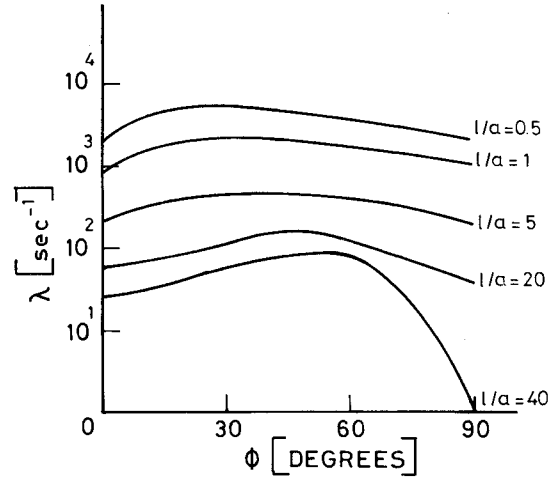

Fig. 3 Effect of fiber winding angle on frequencies of UHMG cylindrical shells; simply supported-simply supported boundary conditions.

Table 1 Natural frequencies of UHMG cylindrical shells having different fiber orientation: $a/h = 100$

	Clamped-clamped; $u = v = w = w_\xi = 0$				
ϕ	0 deg	30 deg	45 deg	60 deg	90 deg
ℓ/a	$\lambda \times 10^{-1}$	$\lambda \times 10^{-1}$	$\lambda \times 10^{-1}$	$\lambda \times 10^{-1}$	$\lambda \times 10^{-1}$
0.5	330(5)[a]	570(5)	500(4)	440(3)	233(3)
1	100(3)	260(3)	200(3)	197(3)	170(3)
2	45.0(3)	120(3)	118(3)	120(3)	59.7(3)
5	26.5(3)	42.9(3)	49(3)	482(3)	31.1(2)
10	10.3(3)	20.8(3)	25.6(3)	25.2(2)	16.5(2)
20	6.60(3)	12.1(2)	15.5(2)	13.2(2)	9.92(1)
30	5.13(2)	9.88(2)	10.6(2)	10.5(2)	5.68(1)
40	3.89(2)	6.91(2)	8.11(2)	9.18(1)	3.61(1)

[a] Numbers in brackets denote circumferential mode.

Table 2 Natural frequencies of UHMG cylindrical shells having different fiber orientation: $a/h = 100$

	Simply supported-simply supported: $v = w = N_\xi = M_\xi = 0$				
ϕ	0 deg	30 deg	45 deg	60 deg	90 deg
ℓ/a	$\lambda \times 10^{-1}$	$\lambda \times 10^{-1}$	$\lambda \times 10^{-1}$	$\lambda \times 10^{-1}$	$\lambda \times 10^{-1}$
0.5	195(9)[a]	459(6)	381(4)	351(4)	190(5)
1	80.7(8)	182(4)	171(4)	167(4)	101(4)
2	43.1(7)	117(4)	11.8(3)	104(3)	51.6(3)
5	19.7(5)	38.7(3)	40.0(3)	39.8(3)	18.9(2)
10	10.6(4)	17.6(3)	20.8(3)	18.9(2)	11.3(2)
20	5.35(3)	11.1(3)	15.2(2)	11.3(2)	3.28(1)
30	3.39(2)	9.51(2)	10.0(2)	9.99(2)	1.35(1)
40	2.32(2)	6.78(2)	7.97(2)	8.65(1)	0.54(1)

[a] Numbers in brackets denote circumferential mode.

C. Approximate Solution of the Transformed Displacement Equations

Despite the existence of an exact solution to the displacement equations of motion, Eq. (5), it might be computationally more convenient to obtain an approximate solution using a finite-difference method. When the free vibrational frequencies are sought, locating the roots of the determinantal equation for λ (from the analytic approach) can be a lengthy process if no order-of-magnitude estimate is available to initialize the search. On the other hand, a finite-difference approach yields fair estimates of many eigenvalues directly, the number of frequencies calculated being proportional to the number of mesh points utilized. Ideally, a combination of the two methods is desirable.

The starting point for the approximate method is the set of transformed equations, Eq. (8). The length of the cylinder is discretized, and the governing equations are written in standard finite-difference forms (see, for example, Fox[10]). The differential equations are thus re-expressed as a set of linear algebraic equations of the form

$$(\boldsymbol{L}^{(n)} - \Omega^2 \boldsymbol{I})\boldsymbol{U}^{(n)} = 0 \tag{13}$$

where $\boldsymbol{L}^{(n)}$ is a matrix whose elements are combinations of coefficients of the $L_{ij}^{(n)}$ and finite-difference weights, $\boldsymbol{I}$ is the identity matrix, and $\boldsymbol{U}^{(n)}$ the vector of discrete transformed displacements. The eigenvalues of the system are determined by demanding that there exists a nontrivial solution, i.e.,

$$\det(\boldsymbol{L}^{(n)} - \Omega^2 \boldsymbol{I}) = 0 \tag{14}$$

Standard computer library programs are readily available for calculating the eigenvalues of a given matrix. In the present work $\boldsymbol{L}^{(n)}$ is recast into Hessenberg form and then its eigenvalues are determined by the QR method of Francis.[11]

IV. Numerical Examples

For the purpose of investigating the effects of filament winding on the free vibrations of single and multilayered shells, the following materials are considered[12]:

1) Ultra high modulus graphite-epoxy (UHMG):

$E_{11} = 3.1 \times 10^{11}$ N/m^2; $E_{22} = 6.2 \times 10^9$ N/m^2;

$E_{66} = 4.1 \times 10^9$ N/m^2; $\nu_{12} = 0.26$ $\rho = 1.6 \times 10^3$ kg/m^3

2) High strength graphite-epoxy (HSG):

$E_{11} = 1.2 \times 10^{11}$ N/m^2; $E_{22} = 1.0 \times 10^{10}$ N/m^2;

$E_{66} = 5.5 \times 10^9$ N/m^2; $\nu_{12} = 0.27$; $\rho = 1.7 \times 10^3$ kg/m^3

For a given fiber orientation, values of the transformed elastic coefficients are calculated from the data using the transformation as given, for example, by Stavsky and Hoff.[13]

In the present work, three sets of boundary conditions are considered (for the notation see Hoff and Soong[14])

RF4-RF4: clamped-clamped, $u = v = w = w_\xi = 0$ at $\xi = 0, \ell/a$

SS3-SS3: simply supported-simply supported, $N_\xi = M_\xi = v = w = 0$ at $\xi = 0, \ell/a$

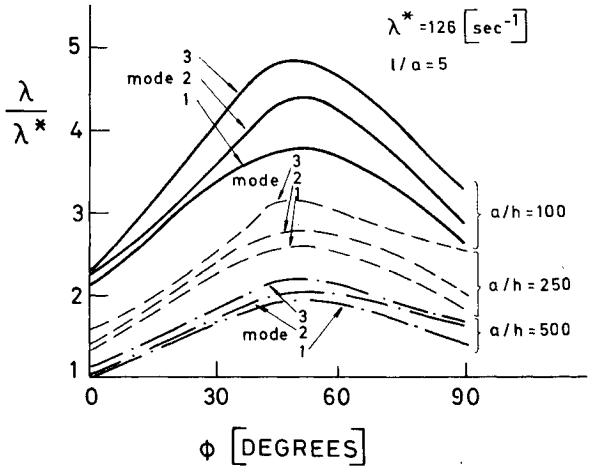

Fig. 4 Effect of fiber winding angle on first three frequencies of UHMG cylindrical shells; clamped-simply supported boundary conditions.

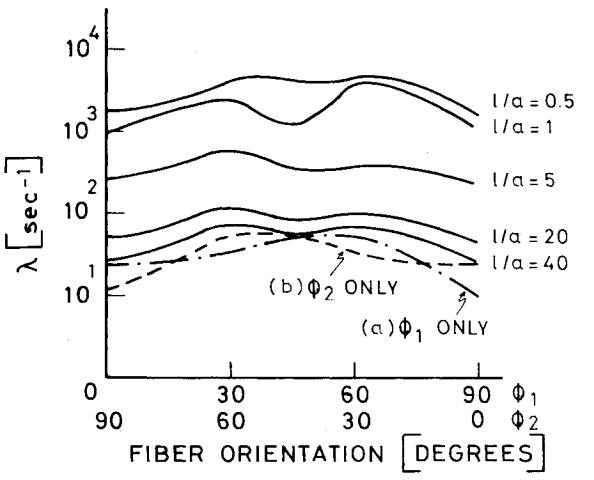

Fig. 5 Effect of fiber winging angles on frequencies of bilayered HSG cylindrical shells; simply supported-simply supported boundary conditions; ϕ_1, ϕ_2 = angles of inner and outer layers, respectively.

Table 3 Natural frequencies of bilayer HSG cylindrical shells; inner and outer layers of equal thickness: $a/h = 100$; SS3-SS3 boundary conditions

$\phi_1 + \phi_2$ [a] $\bar{a}$	0+90 $\lambda \times 10^{-1}$	30+60 $\lambda \times 10^{-1}$	45+45 $\lambda \times 10^{-1}$	60+30 $\lambda \times 10^{-1}$	90+0 $\lambda \times 10^{-1}$
0.5	173(8)[b]	416(0)	399(4)	480(0)	171(8)
1	97(7)	248(4)	115(4)	382(3)	94.2(7)
2	53.3(5)	166(3)	81.2(4)	186(2)	51.5(5)
5	23.5(4)	58.4(3)	33.6(3)	36.9(2)	22.5(4)
10	11.8(3)	21.8(3)	16.0(3)	17.5(2)	11.3(3)
20	4.96(2)	12.8(2)	8.02(2)	11.3(2)	4.71(2)
30	3.82(2)	8.88(1)	6.09(2)	8.66(1)	3.66(2)
40	2.71(1)	7.42(1)	5.53(2)	7.23(1)	2.70(1)

[a] ϕ_1, ϕ_2 are fiber winding angles of inner and outer layers, respectively. [b] Numbers in brackets denote circumferential mode.

RF4-SS3: clamped-simply supported, $u = v = w = w_\xi = 0$ at $\xi = 0$, $N_\xi = M_\xi = v = w = 0$ at $\xi = \ell/a$.

A. Single-Layered Shells

The effect of fiber orientation upon the fundamental frequency of vibration of a single-layered shell is considered. The spectra of lowest frequencies of a UHMG shell, for different winding angles, are illustrated in Fig. 2 (fully clamped boundary conditions) and Fig. 3 (fully simply supported). Actual numerical values together with the appropriate circumferential mode to which the fundamental frequency relates are presented in Tables 1 and 2. The radius to thickness ratio is 100. It is interesting to note the existence of an optimal winding angle for each ℓ/a ratio. For this angle of orientation, the ratio of the free vibrational frequency to that of a shell composed of the same material, but with regular orthotropic orientation, attains a maximum. For example, an increase of about 70% can be obtained for a short, fully clamped shell ($\ell/a = 0.5$) by winding the fibers at 30 deg. For the same simply supported shell the corresponding increase induced is about 150%. Furthermore, for the long simply supported shell ($\ell/a = 40$) a rather remarkable phenomenon is observed. A comparison of the frequencies for the two regular orthotropic limits ($\phi = 0$ and 90 deg) reveals that the frequency for $\phi = 0$ deg is many times larger than that for 90 deg, despite the fact that the fibers have merely been inverted in the two cases. From Table 2 it is noted that for $\phi = 90$ deg the frequency is already associated with the "beam-type" mode ($n = 1$), whereas for $\phi = 0$ deg the second circumferential mode is the fundamental one. In addition, for this long shell, it is observed from Fig. 3 that the slope of the curve ($d\lambda/d\phi$) increases rapidly within the range $60 \leq \phi \leq 90$ deg. Thus, it is concluded that, for large ℓ/a, precision in the angle of winding the fibers is essential because imperfections of a few degrees can considerably alter the vibrational response of the shell.

The change rendered by moving from regular to general orthotropy is not only reflected in numerical differences between frequencies. As evidenced by Tables 1 and 2 the circumferential mode of vibration supplying the natural frequency may also be altered. No definite pattern of dependence of the fundamental mode number upon the winding angle is deducible. However, the tendency appear to be a shift from higher mode numbers at smaller angles to lower mode numbers at higher angles. Ultimately, for very large ℓ/a values the beam-type mode will uniformly provide the lowest frequency.

Consider, now, a UHMG shell that is clamped at one end and simply supported at the other end. In Fig. 4 the influence of fiber orientation on the first three modes of vibration is shown for three different radius to thickness ratios. Note that the optimal winding angles of the lowest and third modes are approximately the same, whereas for the second mode the optimum is slightly higher by between 5-15 deg. Also, if the increase factor I is defined as the ratio between the frequency at the optimum angle to that of the $\phi = 0$ deg orientation then it is found that

1) For $a/h = 100$

$$I_{\text{mode 1}} = 1.78; I_{\text{mode 2}} = 1.91; I_{\text{mode 3}} = 2.10$$

2) For $a/h = 250$

$$I_{\text{mode 1}} = 1.92; I_{\text{mode 2}} = 2.00; I_{\text{mode 3}} = 2.02$$

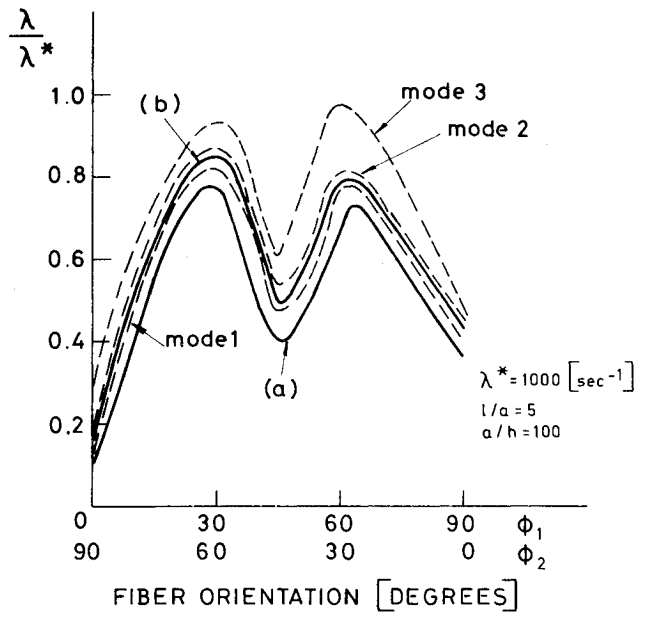

Fig. 6 Effect of fiber winging angles on first three frequencies of bilayered UHMG cylindrical shells: ϕ_1, ϕ_2 = angles of inner and outer layers respectively; – – – RF4-SS3 boundary conditions (a) SS3-SS3 boundary conditions (mode 1 only), (b) RF4-RF4 boundary conditions (mode 1 only).

3) For $a/h = 500$

$$I_{\text{mode 1}} = 1.94; I_{\text{mode 2}} = 1.98; I_{\text{mode 3}} = 1.92$$

Evidently, increased efficiency is obtained for the fundamental mode as the shell thickness is reduced. On the other hand, the converse effect is achieved for the third vibrational mode for which the efficiency decreases under identical circumstances. However, for the thinnest shell considered the best efficiency stems from the second mode.

These results indicate the sensitivity of the vibrational response of both the lowest and higher modes of vibration to the material winding angle and shell geometry.

B. Effect of Fiber Orientation in a Single Material, Bilayered Shell

Consider a shell composed of two equally thick layers of HSG, such that the orientation of the fibers of the inner layer is ϕ_1, and that of the outer layer is ϕ_2. It is assumed that the sum of these angles is 90 deg. The natural frequencies and fundamental mode numbers of various combinations of ϕ_1 and ϕ_2 are listed in Table 3 for a fully simply-supported shell. Some selected results are also presented graphically in Fig. 5. The curves drawn with broken lines around the profile for $\ell/a = 40$ correspond to the profiles that a single-layered HSG shell with orientation ϕ_1 (curve *a*) or ϕ_2 (curve *b*) produce. The form of all the curves for these bilayered shells is very similar, with two conspicuous maxima, and a single minimum at 45 deg (for the latter case the shell is essentially single-layered). The occurrence of the maxima and comparison with curves *a* and *b* indicates that the construction of shells of a single material in this "split" way can lead to higher material frequencies than those of a corresponding single-layered shell with fibers wound at either ϕ_1 or ϕ_2. For the range of combinations examined here, it was found that the aforementioned effect involved factors as high as 3.1 (this occurred for $\ell/a = 2$, $\phi_1 + \phi_2 = 30$ deg).

Suppose a UHMG shell is constructed in the same split way. The shell is clamped at one end and simply supported at the other. The behavior of the first three vibrational frequencies as functions of the winding angles is shown in Fig. 6. Although the two "humps" are evident for all the modes, the maximum frequencies for the first two modes occur with a 30 + 60 deg combination, whereas for the third mode it is the 60 + 30 deg combination that is optimal. For the latter case the efficiency factor is 1.92 (relative to a single-layered shell with $\phi = 30$ deg), but for the 30 + 60 deg combination the efficiency is even higher, being 1.97 for the second mode and 1.94 for the fundamental mode. For comparative purposes, the profiles obtained for the fundamental model of a completely simply supported (curve *a*) and a completely clamped shell (curve *b*) are also shown in Fig. 6. The profile for the RF4-SS3 conditions is closer to the fully clamped shell's profile. The largest difference relative to the fully simply supported case is at the $\phi_1 = \phi_2 = 45$ deg winding angles where a factor of about 1.2 is involved. Thus, control of frequency response via different boundary conditions is also illustrated.

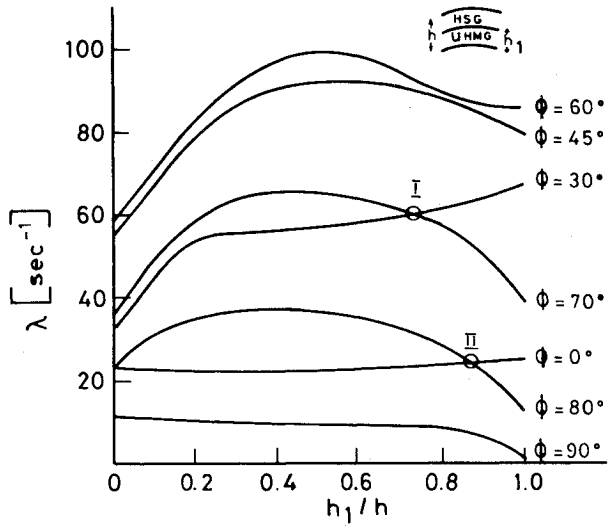

Fig. 7 Effect of relative thickness and fiber winding angle on frequencies of bilayered UHMG/HSG simply supported-simply supported cylindrical shells; $\ell/a = 40$.

C. Effects of Relative Layer Thickness in Bilayered Composite Shells

Let a two-layered shell be composed of an inner layer of UHMG and outer layer of HSG. Let h_1/h be the relative thickness of UHMG; this ratio will be allowed to vary between zero and one. The fibers of the two materials are orientated at the same angle. The dependence of the natural frequency of such a shell upon h_1/h and a variety of values of ϕ is illustrated in Fig. 7 (for $\ell/a = 40$, $a/h = 100$). It is an established fact that for orthotropic composite shells certain combinations of relative thicknesses can provide a higher natural frequency than can be attained by an equivalent homogeneous shell of any of the constitutent materials.[3] The results of Fig. 7 show that such an effect can be induced by simply altering the fiber orientation of the constitutent materials. For $\phi = 0$ deg the frequency response is virtually independent of the amount of UHMG present. At $\phi = 30$ deg the frequency curve rises monotonically from the homogeneous HSG shell frequency to that of a homogeneous UHMG shell.

For the present layup of materials, the angle of 60 deg appears to be optimal in that it provides the highest natural frequencies obtainable for all values of h_1/h and ϕ. Furthermore, for the 60 deg orientation itself, there is an optimal combination of thicknesses, viz., $h_1/h = 0.45$, for which the increased vibrational efficiency factor

$$F_e = \lambda_{\max}/\lambda_{\text{UHMG only}} = 1.2 \tag{15}$$

The aforementioned effect is true for angles of 45, 70, and 80 deg too, for which F_e assumes the values 1.2, 1.63, and 1.6, respectively. Note, also, that for the shell having 74% UHMG

Table 4 Layer thicknesses, winding angles, and stiffness coefficients of various HSG shells

Case	Thicknesses h_1/h	h_2/h	h_3/h	Angles ϕ_1	ϕ_2	ϕ_3	$A_{\xi s}$	$A_{\theta s}$	$B_{\xi s}$	$B_{\theta s}$	$D_{\xi s}$	$D_{\theta s}$
a[a]	0.25	0.5	0.25	45	−45	45	0	0	0	0	0	0
b	0.25	0.5	0.25	45	−45	45	0	0	0	0	+	+
c	0.25	0.5	0.25	−45	45	−45	0	0	0	0	−	−
d	0.5	0.5	0	45	−45	−	0	0	+	+	0	0
e	0.5	0.5	0	−45	45	−	0	0	−	−	0	0
f	1	0	0	45	−	−	−	−	0	0	−[b]	−[b]
g	1	0	0	−45	−	−	+	+	0	0	+[b]	+[b]

[a] $D_{\xi s}$, $D_{\theta s}$ assumed zero (quasiorthotropy assumption). [b] Actual values different from b and c.

Table 5 Frequencies relative to quasiorthotropic case a

ℓ/a	0.5	1	2	5	10	20	40
$\lambda_{b,c}/\lambda_a$	1.1	1.35	1.25	1.02	1.0	1.0	1.0
$\lambda_{d,e}/\lambda_a$	1.1	1.7	2.4	2.0	2.3	1.7	1.7
$\lambda_{f,g}/\lambda_a$	1.4	1.05	1.6	1.6	2.0	1.7	3.2

Table 6 Variation of first lowest frequency; $\ell/a = 5$, $a/h = 100$; material: HSG; simply supported-simply supported boundary conditions

n[a]	Orthotropic $\phi = 0$ deg $\lambda \times 10^{-3}$	$\phi = 45$ deg $\lambda \times 10^{-3}$	$\phi = 90$ deg $\lambda \times 10^{-3}$	Isotropic First $\lambda \times 10^{-3}$	Second $\lambda \times 10^{-3}$
0	1.16	1.38	1.16	3.33	0.963
1	0.765	0.971	0.519	1.66	0.478
2	0.430	0.508	0.215	0.677	0.196
3	0.266	0.336	0.218	0.392	0.113
4	0.202	0.340	0.375	0.427	0.123
5	0.211	0.422	0.599	0.620	0.179
6	0.270	0.512	0.877	0.890	0.257
7	0.358	0.598	1.21	1.22	0.351
8	0.464	0.682	1.59	1.60	0.461
9	0.587	0.598	2.02	2.03	0.585

[a] Circumferential mode.

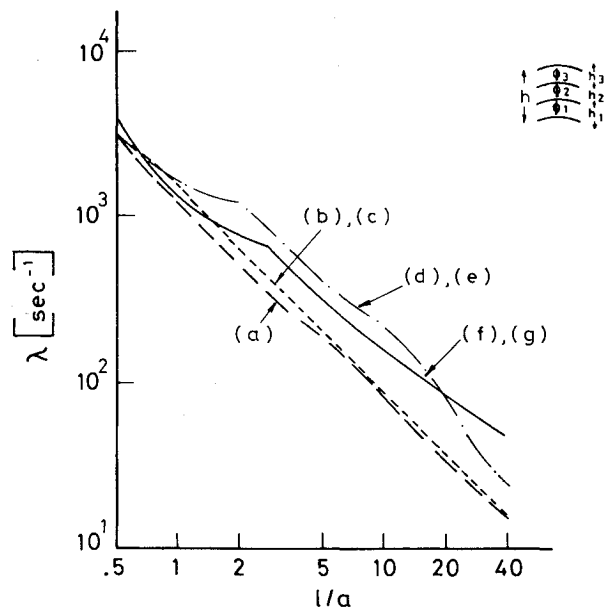

Fig. 8 Frequency envelopes for various single, bi- and tri-layered HSG simply supported-simply supported cylindrical shells.

the same frequency response is obtained for fiber orientation of 30 or 70 deg (point I in Fig. 7). A similar remark is applicable to the shell having 87% UHMG (point II).

Finally, for $\phi = 90$ deg, the frequency curve (in Fig. 7) drops monotonically with $\lambda(\phi = 90 \text{ deg}) < \lambda(\phi = 0 \text{ deg})$ for all thickness combinations. Thus, the frequency response of these layered shells can be controlled by selecting suitable combinations of relative thickness and winding angle.

D. Trilayered and Other Composite Shells

Some filament-wound composite shells are made of three layers of the same material such that the fiber orientations in and relative thicknesses of each layer are as listed in Table 4. Each of the listed elements of the stiffness coefficients matrix is either zero, plus or minus a certain value (denoted by 0, +, −). The unlisted elements are the same for all cases. In order to estimate the frequency of shell b the assumption of quasiorthotropy is made, i.e., the two elements $D_{\xi s}$ and $D_{\theta s}$ are set equal to zero (see Hirano[15] where such an approach is used to estimate buckling loads); the quasiorthotropic shell is shell *a*.

In the present work this assumption is examined and, in addition, various other shells (c-g) having the same amount of the same material are investigated for comparative purposes.

The frequency envelopes for the various HSG shells with simply supported boundary conditions are presented in Fig. 8. In all cases of reversal of the fiber orientations (i.e., b and c, d and e, f and g) the differences in the frequency response are negligible. The frequency envelope for shell *a* appears to be the lower bound of the envelopes. The frequencies of the other shells are tabulated in Table 5 relative to the lower bound. Other than for the longest and shortest shells the most desirable composite is the bilayered combination. Note that for $\ell/a>2$ shell a is an excellent approximation for shell b. However, for $\ell/a<2$ the approximation breaks down and an exact analysis is essential. These results also serve to exemplify the possible sensitivity of the natural frequencies to minor alterations of the stiffness coefficients matrix, for shells comprised of equal amounts of the same material but with different layups and fiber orientation.

As an indication of the possible variation of the first lowest frequency with increasing number n of circumferential waves, and the way in which orientation of the material fiber can be advantageously utilized, results are given in Table 6 for an HSG shell having $\ell/a=5$. Shown also are the frequency spectra of two "isotropic" shells of HSG constructed such that $E_{11}=E_{22}=1.2\times10^{11}$ N/m^2 in the first instance, and $E_{11}=E_{22}=1.0\times10^{10}$ N/m^2 in the second. Note, first of all, that for all the shells the lowest frequencies decrease initially as n increases, reach a minimum, and then increase as n is further increased. This behavior is in accord with the findings of Arnold and Warburton.[16]

The natural frequency of each shell is given by the minimum value in each column. It is interesting to observe that the most efficient shell (in the sense of having the highest natural frequency) is the first isotropic shell. However, if the shell is manufactured orthotropically (i.e., using less material in the θ direction) and the fibers are wound at 45 deg the natural frequency is only reduced by about 10%. On the other hand, reference to Fig. 8 shows again that for shells d and e the natural frequency (for $\ell/a=5$) is about 4×10^2 s^{-1}, i.e., higher than that of the first isotropic shell. In contradistinction, the regular orthotropic and second isotropic shells are clearly not contenders here for maximum vibrational efficiency.

V. Conclusions

A viable approach to the study of the vibrational characteristics of multilayered filament-wound composite shells according to Love type theory is presented. It is of practical interest in that it provides a framework for carrying out parametric-optimization studies of composite shells. The numerous computed results highlight the way in which careful manipulation of fiber winding and/or shell heterogeneity can be advantageously used for obtaining more efficient vibrational responses.

Appendix

The functional differential operators L_{ij} are given by

$$L_{11}=2A_{s\xi}(),_{\xi\theta}+A_{ss}(),_{\theta\theta}+A_{\xi\xi}(),_{\xi\xi}+\Omega^2()$$

$$L_{12}=[A_{ss}+A_{\xi\theta}-\frac{1}{a}(B_{\xi\theta}+2B_{ss})]().,_{\xi\theta}$$
$$+\left(A_{s\theta}-\frac{B_{s\theta}}{a}\right)(),^{B}_{\theta\theta}+\left(A_{\xi s}-\frac{2B_{\xi s}}{a}\right)(),_{\xi\xi}$$

$$L_{13}=-\frac{B_{\xi\xi}}{a}(),_{\xi\xi\xi}-\frac{B_{s\theta}}{a}(),_{\theta\theta\theta}-\frac{3B_{s\xi}}{a}(),_{\xi\xi\theta}$$
$$-\frac{1}{a}(2B_{ss}+B_{\xi\theta})(),_{\xi\theta\theta}-A_{s\theta}(),_{\theta}-\left(A_{\xi\theta}+\frac{\Omega^2}{a}\frac{R_1}{R_0}\right)(),_{\xi}$$

$$L_{21}=[A_{ss}+A_{\xi\theta}-\frac{1}{a}(B_{\xi\theta}+B_{ss})]().,_{\xi\theta}$$
$$+\left(A_{s\theta}-\frac{B_{s\theta}}{a}\right)(),_{\theta\theta}+\left(A_{s\xi}-\frac{B_{s\xi}}{a}\right)(),_{\xi\xi}$$

$$L_{22}=\left(2A_{s\theta}-\frac{5B_{s\theta}}{a}+\frac{3D_{s\theta}}{a^2}\right)(),_{\xi\theta}+\left(A_{\theta\theta}-\frac{2B_{\theta\theta}}{a}+\frac{D_{\theta\theta}}{a^2}\right)(),_{\theta\theta}$$
$$+\left(A_{ss}-\frac{3B_{ss}}{a}+\frac{2D_{ss}}{a^2}\right)(),_{\xi\xi}+\left(1-\frac{3R_1}{aR_0}+\frac{2R_2}{a^2R_0}\right)\Omega^2()$$

$$L_{23}=\frac{1}{a}\left(-B_{s\xi}+\frac{D_{s\xi}}{a}\right)(),_{\xi\xi\xi}+\frac{1}{a}\left(-B_{\theta\theta}+\frac{D_{\theta\theta}}{a}\right)(),_{\theta\theta\theta}$$
$$-\frac{1}{a}[B_{\theta\xi}+2B_{ss}-\frac{1}{a}(D_{\theta}+2D_{ss})](),_{\xi\xi\theta}$$
$$+\frac{3}{a}\left(-B_{\theta s}+\frac{D_{\theta s}}{a}\right)(),_{\xi\theta\theta}+\left[-A_{\theta\theta}+\frac{B_{\theta\theta}}{a}+\Omega^2\right.$$
$$\left.\times\left(-\frac{R_1}{aR_0}+\frac{R_2}{a^2R_0}\right)\right](),_{\theta}+\left(-A_{s\theta}+\frac{B_{s\theta}}{a}\right)(),_{\xi}$$

$$L_{31}=-L_{13}$$

$$L_{32}=\frac{1}{a}\left(B_{\xi s}-\frac{2D_{\xi s}}{a}\right)(),_{\xi\xi\xi}+\frac{1}{a}\left(B_{\theta\theta}-\frac{D_{\theta\theta}}{a}\right)(),_{\theta\theta\theta}$$
$$+\frac{1}{a}[2B_{ss}+B_{\xi\theta}-(4D_{ss}+D_{\xi\theta})/a](),_{\xi\xi\theta}$$
$$+\frac{1}{a}\left(3B_{s\theta}-\frac{4D_{s\theta}}{a}\right)(),_{\xi\theta\theta}+\left(A_{\theta\theta}-\frac{B_{\theta\theta}}{a}+\frac{2R_2}{a^2R_0}\Omega^2\right)(),_{\theta}$$
$$+\left(A_{\theta s}-\frac{2B_{\theta s}}{a}\right)(),_{\xi}$$

$$L_{33}=-\frac{D_{\xi\xi}}{a^2}(),_{\xi\xi\xi\xi}-\frac{D_{\theta\theta}}{a^2}(),_{\theta\theta\theta\theta}-\frac{2}{a^2}(2D_{ss}+D_{\theta\xi})(),_{\xi\xi\theta\theta}$$
$$-\frac{4}{a^2}D_{\theta s}(),_{\xi}-\frac{4}{a^2}D_{s\xi}(),_{\xi\xi\xi\theta}-\frac{4B_{\theta s}}{a}(),_{\xi\theta}$$
$$+\left(-\frac{2B_{\theta\theta}}{a}-\frac{R_2}{a^2R_0}\Omega^2\right)(),_{\theta\theta}+\left(\frac{2B_{\theta\xi}}{a}-\frac{R_2}{a^2R_0}\Omega^2\right)(),_{\xi\xi}$$
$$+(-A_{\theta\theta}+\Omega^2)()$$

where

$$\Omega^2=R_0(a\lambda)^2$$

Acknowledgments

This study was supported by Technion Research Funds and the Fund for the Advancement of Research. Y. Stavsky appreciates the helpful discussions of results with Professor B. Budiansky of Harvard University and Professors S. B. Dong and L. A. Schmit Jr. of the Mechanics and Structures Department at UCLA.

References

[1] Leissa, A. W., "Vibrations of Shells," NASA SP-288, 1973.

[2] Dong, S. B., "Free Vibrations of Laminated Orthotropic Cylindrical Shells," *Journal of the Acoustical Society of America*, Vol. 44, Dec. 1968, pp. 1628-1635.

[3] Stavsky, Y. and Loewy, R., "On Vibrations of Heterogeneous Orthotropic Cylindrical Shells," *Journal of Sound and Vibration*, Vol. 15(2), March 1971, pp. 235-256.

[4] Kunukasseril, V. X., "Vibration of Multilayered Anisotropic Cylindrical Shells," Rept. WVT-6717, AD-649662, Watervliet Arsenal, Watervliet, N.Y., 1967.

[5] Bert, C. W., Baker, J. L., and Egle, D. M., "Free Vibrations of Multilayer Anisotropic Cylindrical Shells," *Journal of Composite Materials,* Vol. 3, July 1969, pp. 480-499.

[6] Forsberg, K., "A Review of Analytical Methods Used to Determine the Modal Characteristics of Cylindrical Shells," NASA CR-613, Sept. 1966.

[7] Cheng, S. and Ho, B.P.C., "Stability of Heterogeneous Aeolotropic Cylindrical Shells Under Combined Loading," *AIAA Journal*, Vol. 1, April 1963, pp. 892-898.

[8] Bo, B.P.C. and Cheng, S., "Some Problems in Stability of Heterogeneous Aeolotropic Cylindrical Shells Under Combined Loading," *AIAA Journal*, Vol. 1, July 1963, pp. 1603-1608.

[9] Ambartsumyan, S. A., "Theory of Anisotropic Shells," NASA TTF-118, May 1964.

[10] Fox, L., *The Numerical Solution of Two-Point Boundary Value Problems*, Oxford University Press, 1957.

[11] Francis, J.G.F., "The QR Transformation—a Unitary Analogue to the LR Transformation," *The Computer Journal*, Vol. 4, 1961, pp. 265-271.

[12] Vicario, A. A. Jr. and Toland, R. H., "Failure Criteria and Analysis of Structural Components," *Composite Materials*, Vol. 7, Academic Press, New York, 1975, pp. 52-97.

[13] Stavsky, Y. and Hoff, N. J., "Mechanics of Composite Structures," Chap. 1 in *Composite Engineering Laminates*, Dietz, A.G.H., Editor, MIT Press, 1969.

[14] Hoff, N. J. and Soong, T. C., "Buckling of Circular Cylindrical Shells in Axial Compression," *International Journal of Mechanical Sciences*, Vol. 7, 1965, pp. 489-520.

[15] Hirano, Y., "Buckling of Angle-Ply Laminated Circular Cylindrical Shells," *Journal of Applied Mechanics*, Vol. 46, March 1979, pp. 233-234.

[16] Arnold, R. N. and Warburton, G. B., "The Flexural Vibrations of Thin Cylinders," *Proceedings of the Institute of Mechanical Engineers,* Vol. 167, 1953, pp. 62-69.